Research Article

Israel Journal of Chemistry
www.ijc.wiley-vch.de

doi.org/10.1002/ijch.202300032

Synthesis, Characterization, and Reactivity Studies of Bis(β-diketiminate) Zinc(II) Complexes

Philipp Rinke,[a] Helmar Görls,[a] and Robert Kretschmer*[a, b, c]

Dedicated to Professor Helmut Schwarz on the occasion of his 80th birthday

Abstract: Zinc(II) complexes bearing bis(β-diketiminate) ligands with various linker groups and terminal substituents have been synthesized by deprotonation of the related bis(β-diketimine)s with zinc(II) bis[bis(trimethylsilylamide)] and diethyl zinc, respectively. One mononuclear and seven dinuclear zinc(II) complexes could be isolated and fully characterized; their solid-state structures have been determined by means of single-crystal X-ray diffraction analysis. Oxygenation experiments of selected dinuclear ethyl zinc bis(β-diketiminate) complexes afforded a series of novel heteroleptic zinc alkoxide, hydroxide, carbonate, and carboxylate complexes. These findings do not only illustrate the complexity of both the oxygenation of organozinc compounds and the transformation pathways of the thus formed compounds but highlight also the impact of the reaction conditions and variations in the ligand framework.

Keywords: Bis(β-diketiminate) ligands · Dinuclear zinc complexes · Oxygenation · Synergy

1. Introduction

The organometallic chemistry of zinc has witnessed a remarkable transition from Frankland's seminal work on diethyl zinc[1] and the stoichiometric utilization of zinc in the Barbier[2] and Reformatsky[3] reactions towards the widespread application of zinc complexes as catalysts for a variety of valuable organic transformations.[4] The high abundancy and hence low price of zinc paired with its low toxicity and good biocompatibility makes zinc catalysts an appealing alternative to expensive and (eco)toxic noble-metal complexes. As such, zinc complexes are used in various catalytic transformations such as C–C, C–N, and C–O bond formation,[5] ring-opening (co)polymerization[6] but also redox reactions.[7] Furthermore, zinc is found in quite a number of naturally occurring enzymes, which inspired generations of bioinorganic and coordination chemists to develop new zinc(II) complexes aiming to mimic the active site of these potent biological catalysts, with carbonic anhydrase being one of the most powerful examples. In recent years, di- and polynuclear zinc complexes[8] received particular interest as cooperative effects arising from the close proximity of two (or more) metal centres give rise to enhanced catalytic activity and selectivity.[9] Bis(β-diketiminate)s[10] have been identified as valuable ligand scaffolds as they are available by simple synthetic protocols and because the metal-metal interaction is readily tuned by adopting the terminal substituent and/or the bridging group. However, small variations in the ligand system may have substantial impact on the catalytic activity as for example illustrated in the ring-opening copolymerization of epoxides and CO_2[11] as well as the ring-opening polymerization of caprolactone and derivatives.[12] Furthermore, dinuclear zinc(II) bis(β-diketiminate) complexes have also been identified as potent catalysts for the borylation of aryl iodides[13] and show interesting reactivity schemes towards oxygen.[14] Inspired by these findings, we explored the impact of the bridging group and the terminal substituent on the synthetic accessibility of dinuclear zinc(II) complexes in which each zinc centre carries either an additional bis(trimethylsilyamide) or ethyl group.

2. Discussion

Based on the synthetic procedures previously reported for the complexes **2a** and **2b**,[12] the dinuclear complexes **2c-f** have

[a] *P. Rinke, Dr. H. Görls, Prof. Dr. R. Kretschmer*
Institute of Inorganic and Analytical Chemistry, Friedrich Schiller University Jena
Humboldtstraße 8, 07743 Jena, Germany
[b] *Prof. Dr. R. Kretschmer*
Institute of Chemistry, Chemnitz University of Technology
Straße der Nationen 62, 09112 Chemnitz, Germany
[c] *Prof. Dr. R. Kretschmer*
Jena Center for Soft Matter (JCSM), Friedrich Schiller University Jena
Philosophenweg 7, 07743 Jena, Germany
E-mail: robert.kretschmer@chemie.tu-chemnitz.de

Supporting information for this article is available on the WWW under https://doi.org/10.1002/ijch.202300032

been obtained in acceptable to good yield by treatment of the bis(β-diketimine)s **1c-f**[15] with zinc(II) bis[bis(trimethylsilyl)amide], $Zn(HMDS)_2$, in toluene at 110 °C, Scheme 1. In case of the *trans*-cyclohexylene bridged protio-ligand **1c**, the reaction time is crucial with respect of whether the mononuclear complex **mono-2c** or the dinuclear complex **2c** is formed. The former one is obtained after two days in 17% crystalline yield while the latter is obtained after four days in 66% yield. Notably, the formation of **mono-2c** is interesting with respect to the synthesis of heterobimetallic complexes for which suitable precursors are rare. After a simple work-up procedure, all compounds are obtained as colourless crystals, which allowed establishing their molecular solid-state structures by means of single-crystal X-ray diffraction analysis, Figure 1.

In both the mononuclear complex **mono-2c** and the dinuclear complexes **2c-f**, the zinc centres are trigonal planar coordinated, a feature previously reported for **2a** and **2b** as

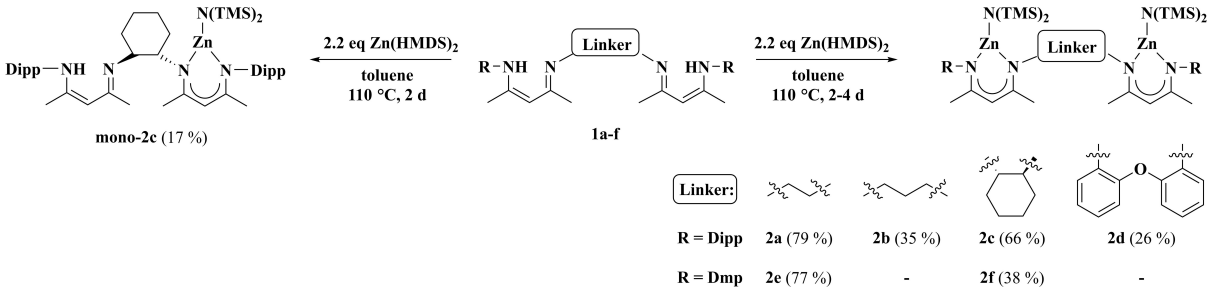

Scheme 1. Syntheses of dinuclear bis(β-diketiminate) zinc bis(trimethylsilylamide) complexes **2a-f** starting from bis(*β*-diketimine)s **1** with different linker groups and zinc(II) bis[bis(trimethylsilyl)amide], $Zn(HMDS)_2$. Dipp = 2,6-diisopropylphenyl, Dmp = 2,6-dimethylphenyl.

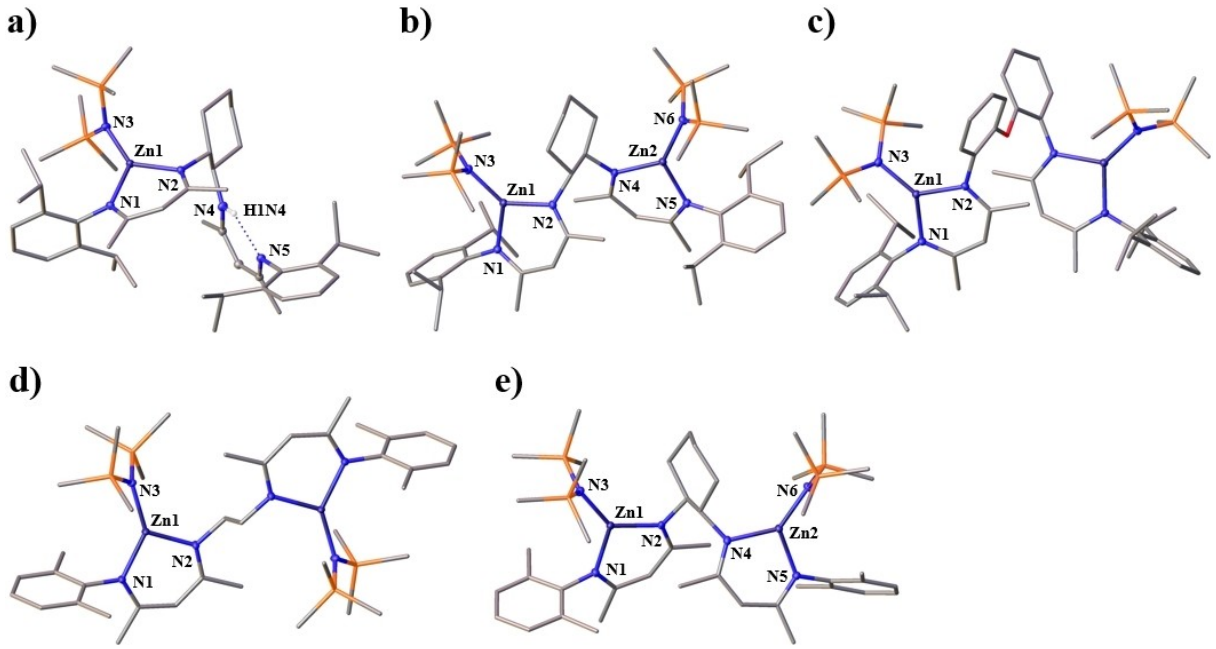

Figure 1. Solid-state molecular structures (hydrogen atoms except the NH in **mono-2c** are omitted for the sake of clarity) with selected bond lengths [Å] and angles [deg]. (a) **mono-2c**: Zn1–N1 1.9638(14), Zn1–N2 1.9682(14), Zn1–N3 1.9041(14), N4–H1 N4 0.85(2), N4–C24 1.353(2), N5–C26 1.299(2), C24–C25 1.369(2), C25–C26 1.441(2), N5···H1 N4 2.0451, N1–Zn1–N2 97.28(6), N1–Zn1–N3 129.39(6), N2–Zn1–N3 133.04(6). (b) 2c: Zn1···Zn2 6.4193(6), Zn1–N1 1.964(3), Zn1–N2 1.977(3), Zn1–N3 1.909(3), Zn2–N4 1.976(3), Zn2–N5 1.973(3), Zn2–N6 1.910(3), N1–Zn1–N2 100.40(13), N1–Zn1–N3 126.87(14), N2–Zn1–N3 132.40(14), N4–Zn2–N5 101.47(14), N4–Zn2–N6 130.97(14), N5–Zn2–N6 126.96(14). (c) 2d: Zn1···Zn1' 7.5424(4), Zn1–N1 1.954(2), Zn1–N2 1.964(2), Zn1–N3 1.885(2), N1–Zn1–N2 98.53(9), N1–Zn1–N3 134.24(9), N2–Zn1–N3 127.13(9). (d) 2e: Zn1···Zn1' 6.4102(4), Zn1–N1 1.9379(12), Zn1–N2 1.9511(11), Zn1–N3 1.8885(11), N1–Zn1–N2 99.09(5), N1–Zn1–N3 137.41(5), N2–Zn1–N3 123.36(5). (e) 2f: Zn1···Zn2 6.2995(5), Zn1–N1 1.9628(13), Zn1–N2 1.9791(13), Zn1–N3 1.8993(13), Zn2–N4 1.9797(13), Zn2–N5 1.9597(13), Zn2–N6 1.9022(13), N1–Zn1–N2 99.49(5), N1–Zn1–N3 126.21(6), N2–Zn1–N3 133.98(6), N4–Zn2–N5 99.66(5), N4–Zn2–N6 134.64(6), N5–Zn2–N6 125.52(6). Symmetry transformations used to generate equivalents atoms (marked with 5'): −x+1, y, −z+1/2 (**2d**); −x+2, −y+1, −z+1 (**2e**).

well as mononuclear β-diketiminate zinc(II) bis(trimethylsilylamide) complexes.[12,16] Similarities are also found with respect to the endocyclic (1.9379(12)–1.9791(13) Å) and exocyclic (1.885(2)–1.910(3) Å) Zn–N bond lengths. In case of **mono-2c**, **2c**, and **2f**, the HMDS groups are tilted toward the terminal substituent as a result of the differing steric constraints of the bridge on one side and the terminal Dipp and Dmp substituents on the other, which results in smaller N1–Zn1–N3 (126.21(6)–129.39(6)°) and larger N2–Zn1–N3 (132.40(14)–133.98(6)°) angles, while in case of **2d** and **2e** the opposite is observed. The Zn···Zn distance increases in the following order: **2f** (6.2995(5) Å) < **2e** (6.4102(4) Å) < **2c** (6.4193(6) Å) < **2d** (7.5424(4) Å).

When repeating the synthesis of **2a** and **2b**, a few crystals have been formed that differ from those of the previously reported zinc(II) bis(β-diketiminate) bis(trimethylsilylamide) complexes **2a** and **2b**. While the low amount of crystalline material was not enough for spectroscopic analyses, the molecular structures in the solid state have been successfully established by single-crystal X-ray diffraction. In fact, the tetranuclear zinc(II) hydroxide complexes **3a** and **3b**, Figure 2, have been serendipitously formed, most likely due to the presence of water during the preparation and subsequent dimerization of the thus formed dinuclear hydroxides. Notably, the synthesis of zinc hydroxides has attracted quite some interest in the last decades due to their relevance in nature and materials sciences. In most of the cases, they are formed by the controlled hydrolysis of zinc alkyls,[17] but such reactions remain challenging and are strongly impacted by the nature of the mono- or multidentate ligand. The molecular structures feature a central $Zn_4(OH)_4$ cycle in a "deck-chair" conformation as previously observed for a tetranuclear indium(III) bis(β-diketiminate) sulphide complex.[18] This finding contrasts the report of an "adamantane-like" fragment as observed for a tetranuclear zinc(II) hydroxide based on a hydrazine-bridged bis(β-diketiminate)[14] and illustrates the impact of the linker group. Two sets of OH groups are located at opposite sides of the eight-membered ring and the respective hydrogen atoms point in opposite direction with respect to each other. The Zn–O (1.9210(15)–1.976(4) Å) and Zn–N (1.9793(15)–1.999(5) Å) bond lengths as well as the O–Zn–O (100.39(7)–113.63(7)°) and N–Zn–N (97.07(17)–100.15(6)°) bond angles are in agreement with previous reports of zinc(II) hydroxide bis- and tris(β-diketiminate)s.[14,19]

The dinuclear zinc ethyl complexes **4a**, **4b**, **4c**, and **4f** were synthesized by deprotonation of the respective protio-ligands **1** with diethyl zinc under inert conditions and obtained in crystalline yields ranging from 35% to 74%, Scheme 2. Please note that the synthesis of **4a** using a different protocol has been reported before.[13] The molecular structures of the complexes **4a**, **4b**, **4c**, and **4f** were determined by single-crystal X-ray diffraction, Figure 3. Their structures feature two tricoordinated zinc centres located within the plane of each NacNac unit. The N–Zn–N bite angles with values between 96.48(13)° and 97.57(8)° and the Zn–C bond lengths (1.961(2)–1.986(3) Å) are in the range typically observed for mono- and dinuclear ethyl zinc(II) β-diketiminate complexes.[13,16] The N1–Zn–C1 and N2–Zn–C1 bond angles are comparable illustrating the lower steric demands of the ethyl group compared to the HMDS substituents in the

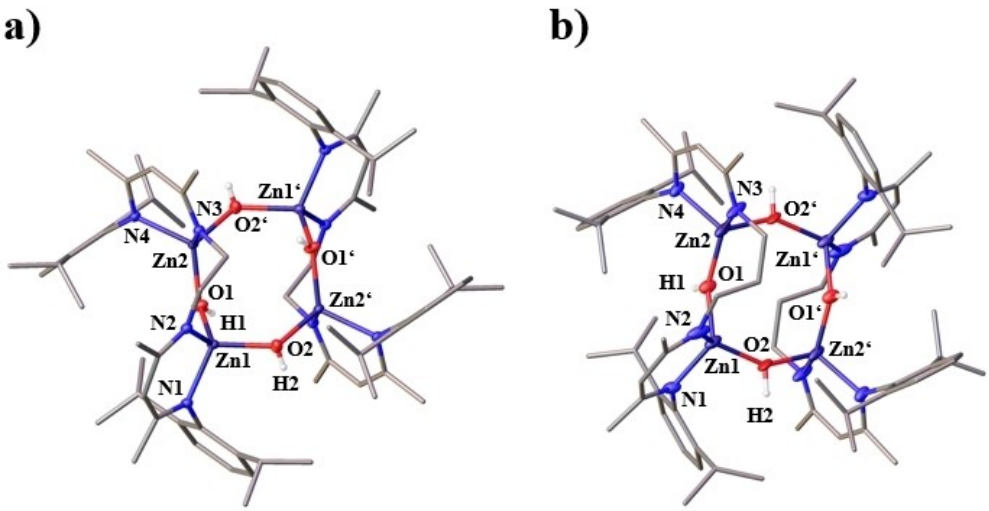

Figure 2. Solid-state molecular structures (hydrogen atoms except the OH are omitted for the sake of clarity) with selected bond lengths [Å] and angles [deg]. (a) **3a**: Zn1···Zn2 3.3312(3), Zn1···Zn2' 3.5817(4), Zn1–N1 1.9836(15), Zn1–N2 1.9793(15), Zn1–O1 1.9709(16), Zn1–O2 1.9533(15), Zn2–N3 1.9852(16), Zn2–N4 1.9906(16), Zn2–O1 1.9210(15), Zn2–O2' 1.9725(15), N1–Zn1–N2 100.15(6), O1–Zn1–O2 100.39(7), N3–Zn2–N4 97.20(6), O1–Zn2–O2' 113.63(7). (b) **3b**: Zn1···Zn2 3.6207(10), Zn1···Zn2' 3.7276(10), Zn1–N1 1.999(5), Zn1–N2 1.990(5), Zn1–O1 1.976(4), Zn1–O2 1.938(4), Zn2–N31.997(4), Zn2–N4 1.983(4), Zn2–O1 1.946(4), Zn2–O2' 1.965(5), N1–Zn1–N2 98.3(2), O1–Zn1–O2 104.92(19), N3–Zn2–N4 97.07(17), O1–Zn2–O2' 103.88(16). Symmetry transformations used to generate equivalents atoms (marked with '): −x+1, −y+1, −z+1 (**3a**); −x+3/2, −y+3/2, −z+1 (**3b**).

Israel Journal of Chemistry

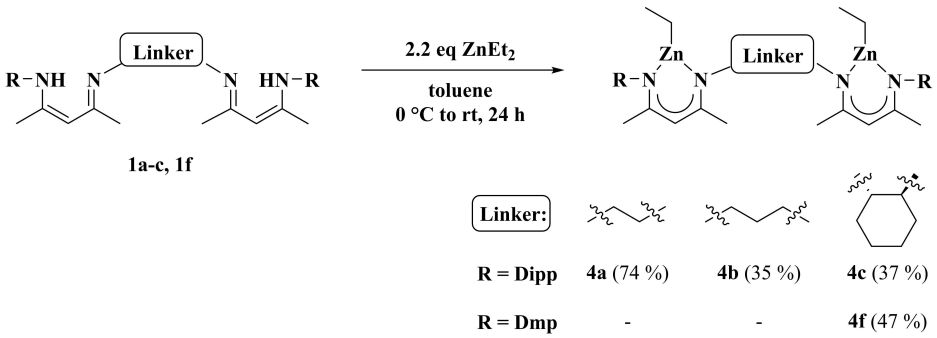

Scheme 2. Syntheses of dinuclear bis(β-diketiminate) zinc ethyl complexes **4a-c** and **4f** starting from bis(*β*-diketimine)s **1** with different linker groups and diethyl zinc. Dipp = 2,6-diisopropylphenyl, Dmp = 2,6-dimethylphenyl.

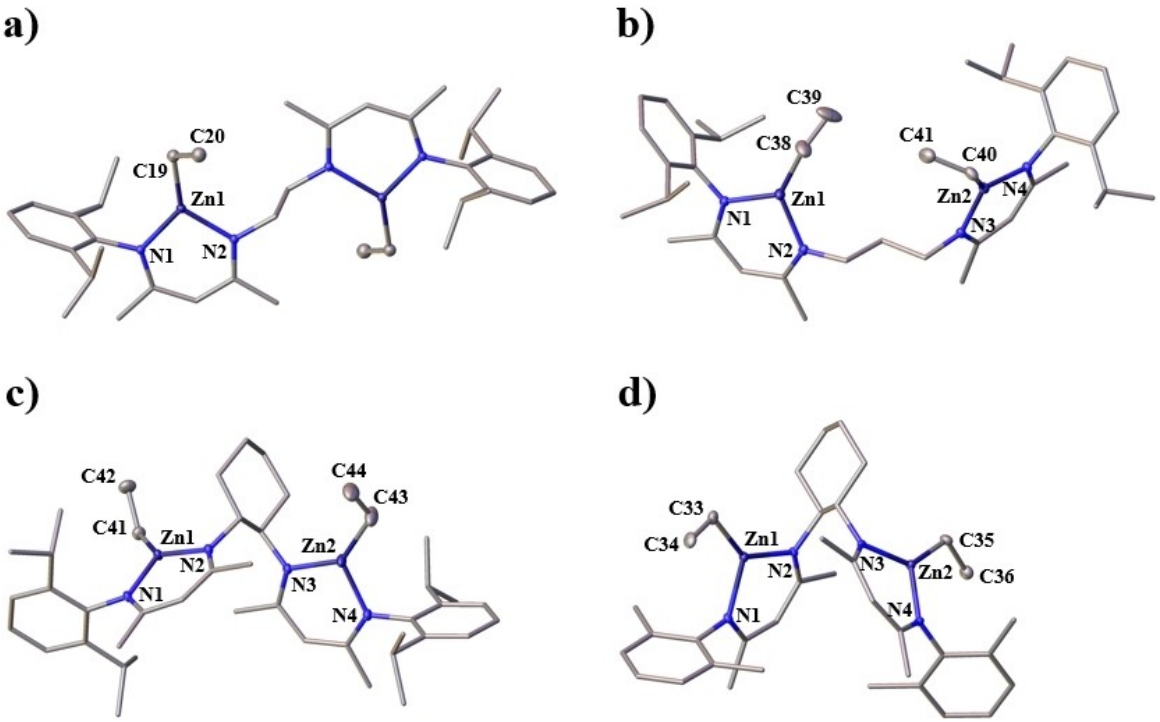

Figure 3. Solid-state molecular structures (hydrogen atoms are omitted for the sake of clarity) with selected bond lengths [Å] and angles [deg]. (a) **4a**: Zn1···Zn1' 6.4509(4), Zn1–N1 1.9531(14), Zn1–N2 1.9588(15), Zn1–C19 1.9679(19), N1–Zn1–N2 96.55(6), N1–Zn1–C19 133.11(7), N2–Zn1–C19 130.14(7). (b) **4b**: Zn1···Zn2 6.4129(5), Zn1–N1 1.9564(16), Zn1–N2 1.9567(16), Zn1–C38 1.967(2), Zn2–N3 1.9630(16), Zn2–N4 1.9495(15), Zn2–C40 1.961(2), N1–Zn1–N2 97.12(7), N1–Zn1–C38 132.59(10), N2–Zn1–C38 130.13(10), N3–Zn2–N4 96.58(6), N3–Zn2–C40 130.89(9), N4–Zn2–C40 132.19(8). (c) **4c**: Zn1···Zn2 5.8164(5), Zn1–N1 1.9630(18), Zn1–N2 1.9739(18), Zn1–C41 1.971(2), Zn2–N3 1.9639(18), Zn2–N4 1.9623(19), Zn2–C43 1.986(3), N1–Zn1–N2 97.36(7), N1–Zn1–C41 124.88(9), N2–Zn1–C41 137.61(9), N3–Zn2–N4 97.57(8), N3–Zn2–C43 139.10(11), N4–Zn2–C41 123.17(11). (d) **4f**: Zn1···Zn2 5.0619(6), Zn1–N1 1.962(3), Zn1–N2 1.962(3), Zn1–C33 1.966(4), Zn2–N3 1.955(3), Zn2–N4 1.957(3), Zn2–C35 1.961(4), N1–Zn1–N2 96.92(13), N1–Zn1–C33 126.43(16), N2–Zn1–C33 136.62(16), N3–Zn2–N4 96.48(13), N3–Zn2–C35 135.34(16), N4–Zn2–C35 127.97(16). Symmetry transformations used to generate equivalents atoms (marked with '): −x+1, −y+1, −z (**4a**).

complexes **2**. Due to packing effects, the Zn···Zn distances in the solid state decrease in the following order **4f** (5.06919(6) Å) < **4c** (5.8164(5) Å) < **4b** (6.4129(5) Å) < **4a** (6.4509(4) and differ slightly from those of the zinc bis(trimethylsilylamide) complexes (**2b** < **2f** < **2c** < **2a**), illustrating the interplay of the bis(β-diketiminate) and the additional ligand.

Inspired by the work of Lewiński and co-workers,[14] we wondered if the synthesis of dinuclear ethyl zinc bis(β-diketiminate) complexes is effected by the presence of dry air. Hence, the reactions of the protio-ligands **1a** and **1b** with

diethyl zinc have been repeated under aerobic conditions, Scheme 3. In case of the ethylene-bridged bis(β-diketimine) **1a**, two new species could be isolated as single crystals in comparable yield. **5a** and **6a** were fully characterized and their solid-state molecular structure was established using X-ray diffraction, Figure 4.

The hexanuclear zinc complex **5a** contains two bis(β-diketiminate) units and formally two sets of tetrahedral coordinated zinc centres, Figure 4a. The first set consists of four Zn atoms that are each chelated by one of the overall four NacNac binding sites. Noteworthily, the coordination geometry differs for each binding pocket of the bis(β-diketiminate). While one zinc atom (Zn1) forms an almost planar ZnN_2C_3

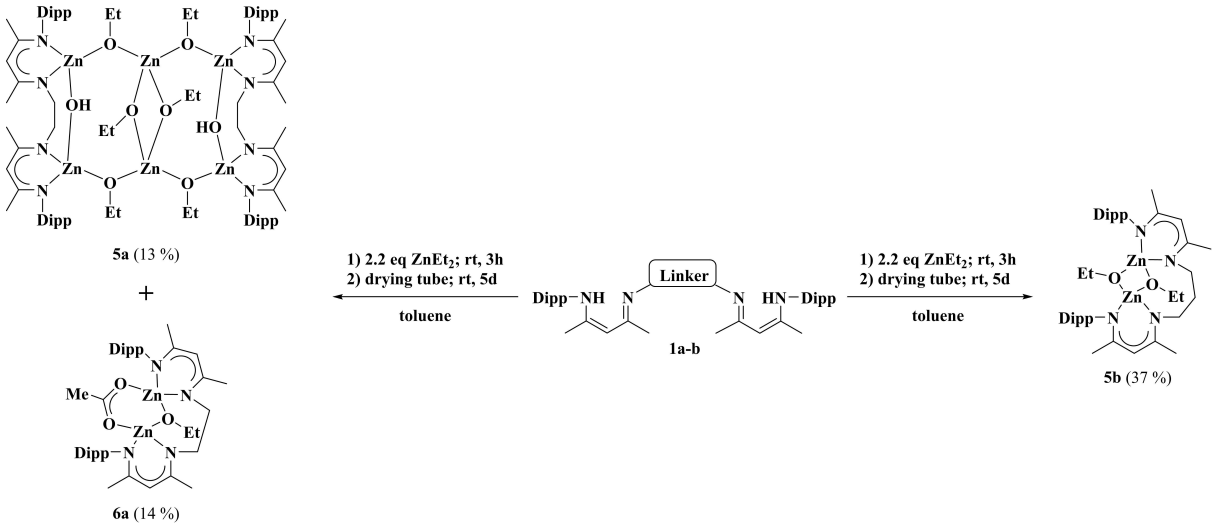

Scheme 3. Reactions of the bis(*β*-diketimine)s **1a** and **1b** with diethyl zinc under aerobic conditions. Dipp = 2,6-diisopropylphenyl.

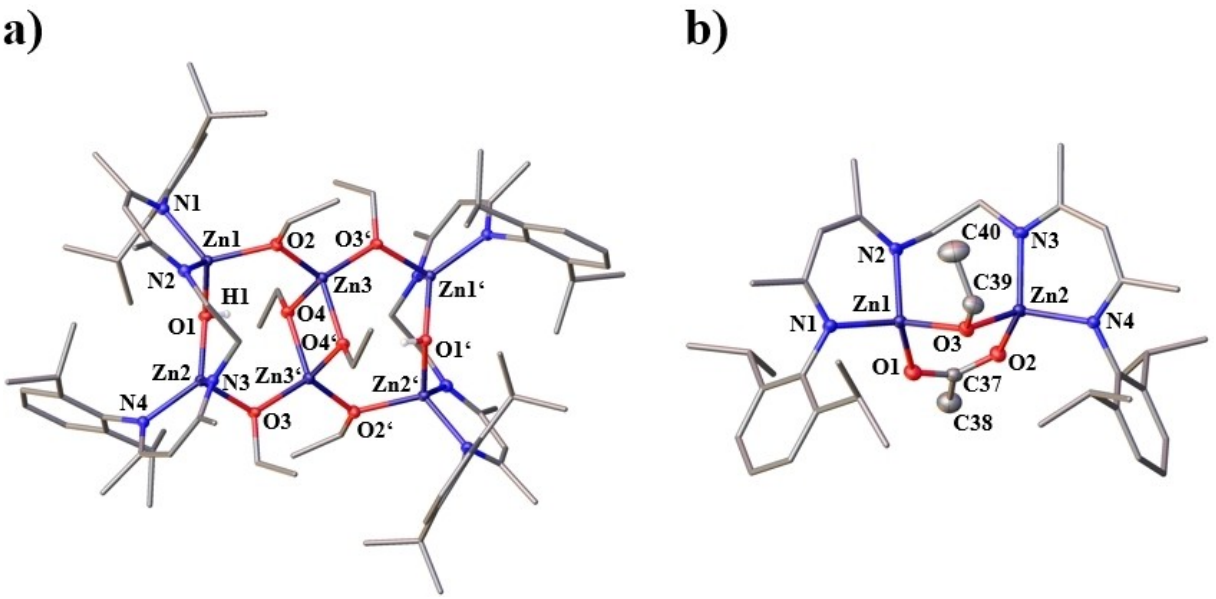

Figure 4. Solid-state structure (hydrogen atoms except the OH in **5a** are omitted for the sake of clarity) with selected bond lengths [Å] and angles [deg]. (a) **5a**: Zn1···Zn2 3.3911(4), Zn1···Zn3 3.4595(5), Zn2···Zn3' 3.4593(5), Zn3···Zn3 3.0002(6), Zn1–N1 1.985(2), Zn1–N2 1.986(2), Zn1–O1 1.9341(17), Zn1–O2 2.0080(17), Zn2–N3 1.990(2), Zn2–N4 1.983(2), Zn2–O1 1.9208(17), Zn2–O3 2.0022(16), Zn3–O2 1.9451(17), Zn3–O3' 1.9330(16), Zn3–O4 2.0120(18), Zn3–O4' 1.9953(17), N1–Zn1–N2 99.49(9), O1–Zn1–O2 101.49(7), N3–Zn2–N4 97.06(8), O1–Zn2–O3 101.77(7), O2–Zn3–O3' 119.00(7), O4–Zn3–O4' 83.05(7). (b) **6a**: Zn1···Zn2 3.0726(7), Zn1–N1 1.953(4), Zn1–N2 1.980(3), Zn1–O1 2.000(3), Zn1–O3 1.957(3), Zn2–N3 1.991(3), Zn2–N4 1.968(3), Zn2–O2 1.987(3), Zn2–O3 1.974(3), O1–C37 1.266(6), O2–C37 1.266(5), C37–C38 1.502(7), N1–Zn1–N2 99.42(15), O1–Zn1–O3 100.30(14), N3–Zn2–N4 100.64(15), O2–Zn2–O3 102.41(13). Symmetry transformations used to generate equivalents atoms (marked with an '): −x+1, −y+1, −z+1 and −x+1, −y+2, −z (**5a**).

ring, the other one resides above the plane of the five-membered N_2C_3-ring. This behaviour also impacts on the N–Zn–N bite angle, which is slightly more obtuse for Zn1 (99.49(9)°) compared to Zn2 (97.06(8)°). The two zinc atoms framed by the same bis(β-diketiminate) are μ-OH bridged and each of these is connected via a μ-OEt bridge with the central $Zn_2(OEt)_2$ fragment giving an overall "tricyclo[5.5.1.1^{1,7}]tetradecane-like" $Zn_6(OH)_2(OEt)_6$ core hold together by two bis(β-diketiminate)s. The hydrogen atoms of the μ-OH groups are each directed towards one of the oxygen atoms of the central $Zn_2(OEt)_2$ rhomb and the OH···O distances of 1.97(3) Å are indicative of hydrogen bonding. As such, **5a** is a unique example of a polynuclear zinc(II) complex with coexisting ethoxide and hydroxide ligands. The second fraction of crystals contained the mixed dinuclear acetate ethoxide zinc(II) complex **6a**, Figure 4b, whose formation is remarkable as the oxidation of zinc alkyl species usually affords the alkoxide, alkylperoxide or hydroxide complexes as well as oxo-encapsulated clusters[14,20] but gives only in rare cases carboxylates.[21] The two zinc centres are twofold bridged by one acetate and one ethoxide unit, respectively, thus generating a central Zn_2O_3C six-membered ring that is reminiscent of a dinuclear (μ-OMe)(μ,η^2-OAc) zinc complex formed upon the reaction of a zinc acetate β-diketiminate and a zinc methoxide β-diketiminate complex.[22] The similarity is reflected in comparable Zn–N (1.953(4)–1.991(3) Å) and Zn–O (1.957(3)–2.000(3) Å) bond lengths as well as N–Zn–N (99.42(15)–100.64(15)°), Zn1–O3–Zn2 (102.80(14)°), and Zn–O–C (114.8(3)–131.0(3)°) bond angles.

The NMR spectra are complex and possess several overlapping regions which impedes detailed mechanistic studies. However, the mechanism suggested by Lewiński *et al.* – although established for a different system[21a] – seems also feasible in this case: Initially an ethyl peroxide may be formed and undergoes a 1,2-hydrogen shift towards a zinc 2-hydroxy-2-ethoxide, which by dehydrogenation forms the bridging acetate complex. Subsequent reaction of the remaining ethyl zinc site than yields the frequently observed ethoxide rest most likely via an alkyl peroxide intermediate. Notably, these are just assumptions and computational chemists might be interested in shedding light into the mechanism of this interesting reaction which most likely benefits from cooperative effects.

With respect to cooperative effects, the linker group also plays an important role in here as the aerobic reaction of the propylene-bridged (β-diketimine) **1b** with diethyl zinc affords the dinuclear ethoxide complex **5b** as the only isolable product, Scheme 3. The central $Zn_2(OEt)_2$ fragment has previously been reported for β-diketiminate complexes which have been accessed either by ethanolysis of a methyl zinc(II) β-diketiminate[23] or a dinuclear zinc(I) β-diketiminate,[24] by oxygenation of an ethyl zinc(II) β-diketiminate[25] or by an oxygen-transfer reaction originating from the respective ethylperoxide zinc(II) complex.[21b] Hence, it is without surprise that the geometric features with respect to the Zn–N (1.9531(15)–1.9866(15) Å and Zn–O (1.9681(12)–1.9868(12) Å bond lengths as well as the N–Zn–N (97.87(6)–97.91(6)°)and O–Zn–O (80.90(5)–81.16(5)°) bond angles are reminiscent of those of the previously reported complexes (Figure 5).

We finally investigated if the reaction of the dinuclear ethyl zinc complex **4a** with dry air also affords **5a** and **6a**. While the crude NMR of the reaction mixture reveals a complex mixture of seemingly several species, a few crystals of two different types could be obtained from a concentrated solution in *n*-hexane at −25°C. They belong to the tetranuclear hydroxide complex **3a** discussed above and to the unique hexanuclear ethoxide zinc carbonate hydroxide complex **7a**, Scheme 4. Within **7a**, four tetrahedral zinc centres are coordinated by two bis(β-diketiminate) units. The two additional zinc atoms are located in the centre of the complex and connected to the other four zinc atoms via overall one carbonate, four ethoxide, and two hydroxide ligands forming an "octahydro-1*H*,4*H*,7*H*-3a,6a-propanophenalene-like" Zn_6O_9C polycycle. While the formation of alkoxide and hydroxide complexes by oxygenation of zinc alkyl complexes has been reported for several examples,[14,20] the incorporation of CO_2 is rather rare.

However, the presence of hydroxide groups hints towards the reaction mechanism as zinc hydroxide complexes have been shown to react with CO_2 by carbonate formation.[26] As

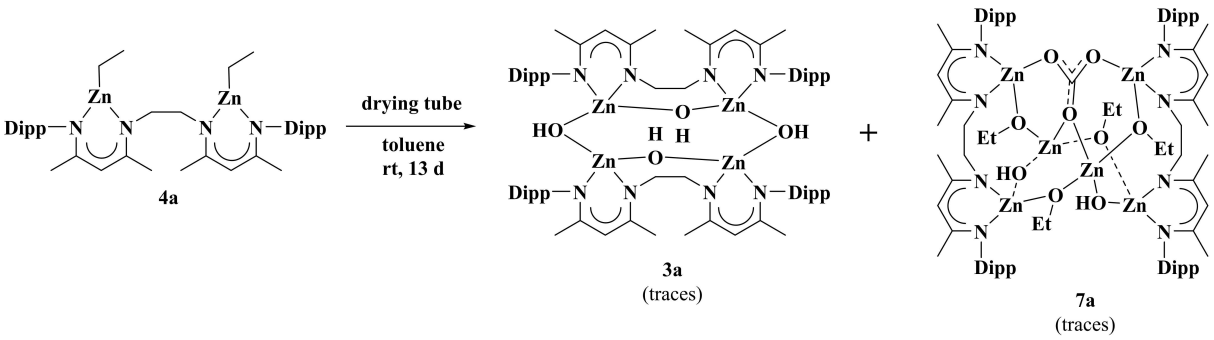

Scheme 4. Reaction of the of dinuclear bis(β-diketiminate) zinc ethyl complex **4a** with dry air. Dipp = 2,6-diisopropylphenyl.

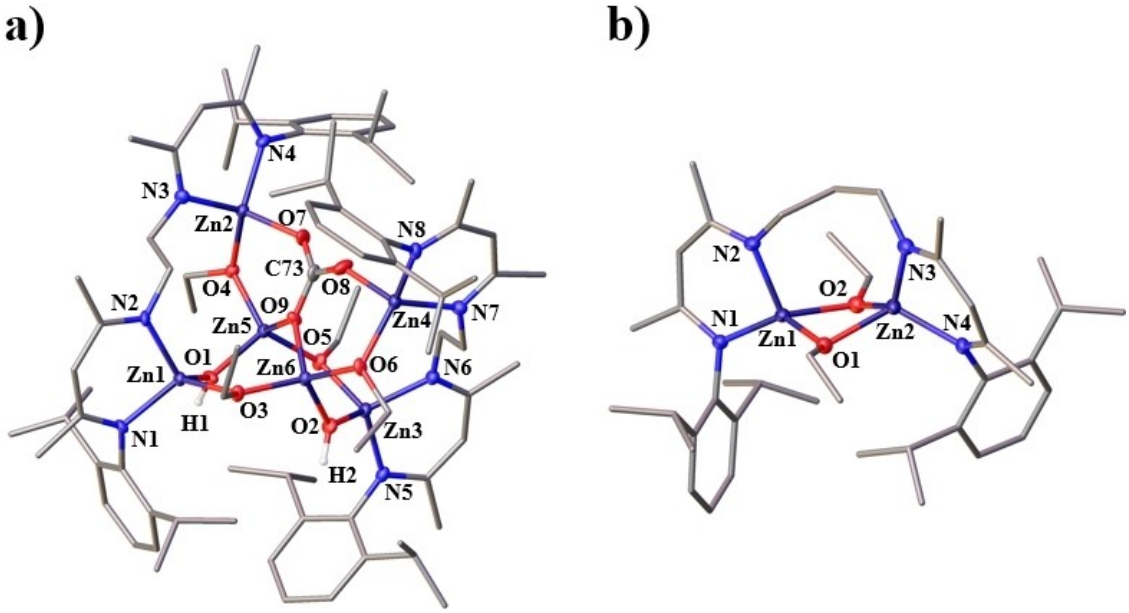

Figure 5. Solid-state molecular structures (hydrogen atoms except the OH in **7a** are omitted for the sake of clarity) with selected bond lengths [Å] and angles [deg]. (a) **7a**: Zn1···Zn2 5.114(1), Zn1···Zn5 3.4713, Zn1···Zn6 3.355(1), Zn2···Zn5 3.204(1), Zn2···Zn6 5.402(1), Zn3···Zn4 5.058(1), Zn3···Zn5 3.371(1), Zn3···Zn6 3.505(1), Zn4···Zn5 5.423(1), Zn4···Zn6 3.281(1), Zn5···Zn6 3.451(1), Zn1–N1 1.968(6), Zn1–N2 1.987(6), Zn1–O1 1.947(5), Zn1–O3 1.987(5), Zn2–N3 1.973(6), Zn2–N4 1.947(7), Zn2–O4 1.948(5), Zn2–O7 1.976(6), Zn3–N5 1.972(6), Zn3–N6 1.967(7), Zn3–O2 1.947(5), Zn3–O5 1.979(5), Zn4–N7 1.960(7), Zn4–N8 1.966(7), Zn4–O6 1.938(5), Zn4–O8 1.972(6), Zn5–O1 1.941(5), Zn5–O4 1.942(5), Zn5–O5 1.918(5), Zn5–O9 2.009(5), Zn6–O2 1.949(5), Zn6–O3 1.902(5), Zn6–O6 1.949(5), Zn6–O9 2.005(5), O7–C73 1.229(10), O8–C73 1.249(10), O9–C73 1.315(10), N1–Zn1–N2 98.1(3), O1–Zn1–O3 104.2(2), N3–Zn2–N4 100.1(3), O4–Zn2–O7 96.1(2), N5–Zn3–N6 98.5(3), O2–Zn3–O5 104.8(2), N7–Zn4–N8 98.9(3), O6–Zn4–O8 97.5(2), O1–Zn5–O5 115.9(2), O4–Zn5–O9 114.1(2), O2–Zn6–O3 112.8(2), O6–Zn6–O9 112.2(2). (b) **5b**: Zn1···Zn2 2.9091(3), Zn1–N1 1.9531(15), Zn1–N2 1.9866(15), Zn1–O1 1.9681(12), Zn1–O2 1.9868(12), Zn2–N3 2.0004(15), Zn2–N4 1.9606(15), Zn2–O1 1.9942(12), Zn2–O2 1.9497(12), N1–Zn1–N2 97.91(6), O1–Zn1–O2 80.90(5), N3–Zn2–N4 97.87(6), O1–Zn2–O2 81.16(5).

such, **7a** serves as a unique example for the incorporation of CO_2 in a polynuclear zinc complex.

3. Conclusions

Using bis(β-diketimine)s **1** with different linker groups, dinuclear zinc(II) bis(trimethylsilylamide) (**2**) as well as dinuclear diethyl zinc(II) complexes (**4**) were synthesized by deprotonation. The complexes have been fully characterized and their molecular solid-state structures were obtained by single-crystal X-ray diffraction analysis. In addition, two tetranuclear zinc(II) hydroxide complexes featuring a central Zn_4O_4 fragment are presented. The presence of dry air during the synthesis of the dinuclear ethyl zinc complexes **4a** and **4b** was probed and gave rise to polynuclear zinc(II) complexes with acetate, ethoxide, and hydroxide bridges. Finally, when **4a** is allowed to react with dry air, the tetranuclear zinc hydroxide complex **3a** is formed besides the hexanuclear complex **7a** carrying overall two bis(β-diketiminate), one carbonate, four ethoxide, and two hydroxide ligands. In light of the results, we think this work is well suited to be dedicated to Professor Helmut Schwarz on the occasion of his 80th birthday. On the one hand because his seminal work on the activation of carbon dioxide by cation zinc hydroxide species in the gas phase[27] is related to the formation of complex **7a**. On the other hand because of his continuing interest in hydrogen-atom transfer (HAT),[28] which is assumed to play a crucial role in the formation of zinc hydroxide complexes from the reaction of zinc alkyls with oxygen.

4. Experimental and Computational Details

General Considerations. All preparations, except the syntheses of **5a**, **5b**, **6a**, and **7a**, have been performed under an inert atmosphere of dinitrogen by means of Standard Schlenk-line techniques, while the samples for analytics were handled in a glovebox (GS-Systemtechnik and MBraun). Yields are not optimized and refer to isolated crystalline material. The crystals were collected, washed with *n*-pentane and dried in vacuum to obtain the products. All solvents (*n*-hexane, *n*-pentane, and toluene) were distilled from sodium/benzophenone prior to use, while C_6D_6 and THF-d_8 were dried using molecular sieves (4 Å). $Zn(HMDS)_2$, **2a**, **2b**, and the protio-ligands **1a-f** have been synthesized according to literature procedures.[12,15]

Characterization. The NMR-spectra were recorded on BrukerAvance 300 and 400 spectrometers (T = 300 K) with δ

(given in ppm) referenced to external trimethylsilane (^{1}H and ^{13}C) and trichlorofluoromethane (^{19}F). ^{1}H and ^{13}C NMR spectra were calibrated using the solvent residual peak (δ ^{1}H (C_6D_5H) = 7.20) and the solvent peak (δ ^{13}C (C_6D_6) = 128.0), respectively. The coupling constants *J* are given in Hertz [Hz]. Elemental analysis were performed on a Vario micro cube (Elementar Analysensysteme GmbH). IR spectra were recorded with a Agilent Cary 630 spectrometer equipped with a diamond ATR unit.

mono-2c: $Zn(HMDS)_2$ (1.3 mL, 3.1 mmol) was added dropwise to a stirred solution of **1c** (850 mg, 1.4 mmol) in toluene (8 mL) at room temperature, followed by stirring at 110 °C for 2 days. After cooling to room temperature, the red-brown solution was filtered. The filtrate was concentrated to three-quarters of the initial volume, and colourless crystals of **mono-2c** (200 mg, 0.2 mmol, 17%) were obtained upon storage at 4.5°C.

^{1}H NMR (300 MHz, C_6D_6): δ = 10.75 (d, $^{3}J_{HH}$ = 8.7 Hz, 1H, N*H*), 7.25–7.11 (m, 6H, Ar*H*), 4.67 (s, 1H, C*H*), 4.59 (s, 1H, C*H*), 3.58–3.50 (m, 1H, ring-C*H*), 3.43–3.31 (m, 2H, ring-C*H* & C*H*Me_2), 3.17–3.01 (m, 3H, C*H*Me_2), 2.53–2.40 (m, 1H, ring-CH_2), 2.04 (br, 1H, ring-CH_2), 1.89 (d, $^{3}J_{HH}$ = 10.1 Hz, 6H, C*Me*), 1.83–1.73 (m, 2H, ring-CH_2), 1.59 (d, $^{3}J_{HH}$ = 8.7 Hz, 6H, C*Me*), 1.53–1.45 (m, 4H, ring-CH_2 & CHMe_2), 1.34–1.12 (m, 24H, ring-CH_2 & CHMe_2), 0.30 (s, 9H, SiMe_3), 0.06 (s, 9H, SiMe_3); ^{13}C{^{1}H} NMR (75 MHz, C_6D_6): δ = 168.51 (*C*N), 166.72 (*C*N), 154.88 (*C*N), 147.34 (*i*-C_{arom}), 145.06 (*i*-C_{arom}), 142.80 (*o*-C_{arom}), 142.30 (*o*-C_{arom}), 138.87 (*o*-C_{arom}), 126.16 (*p*-CH_{arom}), 124.18 (*m*-CH_{arom}), 123.97 (*m*-CH_{arom}), 123.60, 123.40, 123.16, 96.14 (*C*H), 95.56 (*C*H), 64.27 (ring-*C*H), 60.38 (ring-*C*H), 36.07 (ring-*C*H_2), 35.45 (ring-*C*H_2), 29.17 (*C*HMe_2), 28.38 (*C*HMe_2), 28.32 (*C*HMe_2), 28.17 (*C*HMe_2), 26.02 (CHMe_2), 25.35 (ring-*C*H_2), 25.16 (ring-*C*H_2), 24.70, 24.43 (CHMe_2), 24.14 (*C*Me), 24.00 (CHMe_2), 23.97 (*C*Me), 23.89, 23.05, 21.99 (*C*Me), 19.97 (*C*Me), 5.91 (SiMe_3), 5.71 ppm (SiMe_3); ATR-IR: $\tilde{\nu}$ = 3064, 2952, 2925, 2858, 1620, 1549, 1524, 1457, 1434, 1389, 1363, 1318, 1240, 1181, 1111, 1096, 980, 937, 879, 858, 843, 816, 794, 785, 749, 728, 694, 669 cm^{-1}; Anal. calc. (found) for $C_{46}H_{77}N_5Si_2Zn \cdot 0.55\,C_7H_8$: C, 68.63 (68.42), H, 9.40 (9.11), N, 8.03 (8.09).

2c: $Zn(HMDS)_2$ (1.0 mL, 2.5 mmol) was added dropwise to a stirred solution of **1c** (675 mg, 1.1 mmol) in toluene (6 mL) at room temperature. After stirring for 4 days at 110 °C, the dark red solution was cooled down to room temperature, affording colourless crystals of **2c** (780 mg, 0.7 mmol, 66%).

^{1}H NMR (300 MHz, C_6D_6): δ = 7.17–7.15 (m, 6H, Ar*H*), 4.67 (s, 2H, C*H*), 3.94–3.78 (m, 2H, ring-C*H*), 3.29 (sept, $^{3}J_{HH}$ = 6.8 Hz, 2H, C*H*Me_2), 3.13 (sept, $^{3}J_{HH}$ = 6.8 Hz, 2H, C*H*Me_2), 2.96–2.85 (br, 2H, ring-CH_2), 2.18 (s, 6H, C*Me*), 2.11–2.06 (br, 2H, ring-CH_2), 1.98–1.95 (br, 2H, ring-CH_2), 1.49 (s, 6H, C*Me*), 1.43 (d, $^{3}J_{HH}$ = 6.8 Hz, 6H, CHMe_2), 1.37 (br, 2H, ring-CH_2), 1.30 (d, $^{3}J_{HH}$ = 6.8 Hz, 6H, CHMe_2), 1.12 (dd, $^{3}J_{HH}$ = 6.7 & 1.6 Hz, 12H, CHMe_2), 0.33 (s, 18H, SiMe_3), 0.08 (s, 18H, SiMe_3); ^{13}C{^{1}H} NMR (101 MHz, C_6D_6): δ = 169.37 (*C*N), 169.11 (*C*N), 144.39 (*i*-C_{arom}), 142.48 (*o*-C_{arom}), 141.83 (*o*-C_{arom}), 126.11 (*p*-CH_{arom}), 124.13 (*m*-CH_{arom}), 123.76 (*m*-CH_{arom}), 95.36 (*C*H), 66.56 (ring-*C*H), 36.31 (ring-*C*H_2), 28.01 (*C*HMe_2), 27.76 (*C*HMe_2), 25.70 (*C*Me), 25.59 (ring-*C*H_2), 24.87 (CHMe_2), 24.70 (ring-*C*H_2), 24.17 (CHMe_2), 24.02 (*C*Me), 23.80 (CHMe_2), 5.52 (SiMe_3), 5.31 ppm (SiMe_3); ATR-IR: $\tilde{\nu}$ = 2958, 2942, 2861, 1527, 1457, 1435, 1386, 1365, 1317, 1271, 1242, 1189, 1094, 1029, 983, 950, 877, 843, 815, 794, 761, 746, 663 cm^{-1}; Anal. calc. (found) for $C_{52}H_{94}N_6Si_4Zn_2$: C, 59.68 (59.99), H, 9.05 (9.16), N, 8.03 (7.88).

2d: $Zn(HMDS)_2$ (1.3 mL, 3.2 mmol) was added dropwise to a stirred solution of **1d** (1.0 g, 1.5 mmol) in toluene (12 mL) at room temperature, followed by stirring at 110 °C for 3 days. After cooling to room temperature, all volatiles of the orange solution were removed in vacuum. The brown crude product was dissolved in toluene (10 mL), filtered and the filtrate was concentrated to two-thirds of the initial volume. **2d** (425 mg, 0.4 mmol, 26%) was obtained in two fractions from the filtrate as colourless crystals at room temperature.

^{1}H NMR (400 MHz, C_6D_6): δ = 7.33 (dt, $^{3}J_{HH}$ = 7.2 & 2.5 Hz, 4H, ArH_{Linker}), 7.18–7.09 (m, 4H, Ar*H*), 6.96–6.893 (m, 4H, ArH_{Linker}), 5.08 (s, 2H, C*H*), 3.29 (sept, $^{3}J_{HH}$ = 6.7 Hz, 2H, C*H*Me_2), 3.08 (sept, $^{3}J_{HH}$ = 6.8 Hz, 2H, C*H*Me_2), 2.07 (s, 6H, C*Me*), 1.70 (s, 6H, C*Me*), 1.95 (d, $^{3}J_{HH}$ = 6.8 Hz, 6H, CHMe_2), 1.19 (dd, $^{3}J_{HH}$ = 8.2 & 6.8 Hz, 12H, CHMe_2), 1.01 (d, $^{3}J_{HH}$ = 6.8 Hz, 6H, CHMe_2), 0.19 (s, 18H, SiMe_3), −0.07 ppm (s, 18H, SiMe_3); ^{13}C{^{1}H} NMR (101 MHz, C_6D_6): δ = 170.40 (*C*N), 169.85 (*C*N), 149.36, 144.26, 142.35, 142.16, 139.54, 126.61, 125.99, 124.51, 124.33, 123.76, 118.97 (Ar-CH_{Linker}), 96.51 (*C*H), 28.43 (*C*HMe_2), 25.22 (CHMe_2), 24.64 (CHMe_2), 24.59 (CHMe_2), 24.57 (*C*Me), 23.88 (*C*Me), 5.68 (SiMe_3), 5.17 ppm (SiMe_3); ATR-IR: $\tilde{\nu}$ = 2961, 2871, 1532, 1484, 1387, 1369, 1317, 1240, 1202, 1180, 1110, 1026, 990, 940, 881, 845, 827, 816, 797, 759, 744, 729, 669 cm^{-1}; Anal. calc. (found) for $C_{58}H_{92}N_6Si_4OZn_2 \cdot 0.45\,C_7H_8$: C, 62.56 (62.50), H, 8.21 (8.30), N, 7.16 (6.99).

2e: $Zn(HMDS)_2$ (1.7 mL, 4.1 mmol) was added dropwise to a stirred solution of **1e** (800 mg, 1.9 mmol) in toluene (10 mL) at room temperature, followed by stirring at 110 °C for 2 days. After cooling to room temperature, colourless crystals grow from the solution and were separated by filtration to give **2e** (1.3 mg, 1.4 mmol, 77%).

^{1}H NMR (400 MHz, C_6D_6): δ = 7.01–6.93 (m, 6H, Ar*H*), 4.75 (s, 2H, C*H*), 3.86 (s, 4H, CH_2CH_2), 2.24 (s, 6H, C*Me*), 2.15 (s, 12H, Ar*Me*), 1.50 (s, 6H, C*Me*), 0.13 ppm (s, 36H, SiMe_3); ^{13}C{^{1}H} NMR (101 MHz, C_6D_6): δ = 170.40 (*C*N), 167.71 (*C*N), 147.13 (*i*-C_{arom}), 131.93 (*o*-C_{arom}), 128.99 (*m*-CH_{arom}), 125.46 (*p*-CH_{arom}), 96.30 (*C*H), 53.04 (CH_2CH_2), 23.16 (C*Me*), 23.07 (*C*Me), 18.92 (Ar*Me*), 5.26 ppm (SiMe_3); ATR-IR: $\tilde{\nu}$ = 2922, 1625, 1551, 1520, 1474, 1436, 1385, 1367, 1308, 1287, 1252, 1242, 1216, 1195, 1108, 1094, 1025, 984, 875, 858, 844, 823, 810, 796, 763, 748, 669 cm^{-1}; Anal. calc. (found) for $C_{40}H_{72}N_6Si_4Zn_2 \cdot 0.25\,C_7H_8$: C, 55.92 (55.64), H, 8.26 (7.99), N, 9.30 (9.27).

2f: $Zn(HMDS)_2$ (1.1 mL, 2.7 mmol) was added dropwise to a stirred solution of **1f** (600 mg, 1.2 mmol) in toluene (8 mL) at room temperature. After stirring for 2 days at 110 °C, the orange-red solution was cooled to room temperature, filtered and concentrated to three-quarters of the initial volume. **2f** (445 mg,

0.5 mmol, 38 %) was obtained in two fractions from the filtrate as colourless crystals at room temperature.

^{1}H NMR (400 MHz, C_6D_6): δ = 7.04–6.95 (m, 6H, Ar*H*), 4.64 (s, 2H, C*H*), 3.86–3.78 (m, 2H, ring-C*H*), 2.83–2.80 (br, 2H, ring-CH_2), 2.26 (s, 6H, Ar*Me*), 2.15 (s, 6H, C*Me*), 2.11 (s, 6H, Ar*Me*), 2.05–2.01 (br, 2H, ring-CH_2), 1.90–1.87 (br, 2H, ring-CH_2), 1.42 (m, 8H, C*Me* & ring-CH_2), 0.30 (s, 18H, SiMe_3), 0.06 (s, 18H, SiMe_3); ^{13}C{^{1}H} NMR (101 MHz, C_6D_6): δ = 169.42 (*C*N), 168.21 (*C*N), 146.92 (*i*-C_{arom}), 132.56 (*o*-C_{arom}), 131.68 (*o*-C_{arom}), 129.08 (*m*-CH_{arom}), 128.84 (*m*-CH_{arom}), 125.49 (*p*-CH_{arom}), 95.60 (*C*H), 67.10 (ring-*C*H), 36.28 (ring-*C*H_2), 26.61 (*C*Me), 25.23 (ring-*C*H_2), 23.25 (*C*Me), 19.74 (Ar*Me*), 19.38 (Ar*Me*), 6.00 (SiMe_3), 5.51 ppm (SiMe_3);ATR-IR: $\tilde{\nu}$ = 2942, 2852, 1541, 1522, 1457, 1437, 1387, 1360, 1308, 1274, 1261, 1241, 1198, 1084, 1064, 1029, 1015, 982, 879, 843, 812, 764, 750, 667 cm^{-1}; Anal. calc. (found) for $C_{44}H_{78}N_6Si_4Zn_2$: C, 56.57 (56.28), H, 8.42 (8.22), N, 9.00 (8.93).

4a: $ZnEt_2$ (4.5 mL, 4.5 mmol, 1 M in hexanes) was added dropwise to a stirred solution of **1a** (1.1 g, 2.0 mmol) in toluene (10 mL) at 0 °C, followed by stirring at room temperature overnight. The orange Suspension was heated until a clear solution was obtained and slowly cooled down to room temperature, affording colourless crystals of **4a** (1.1 g, 1.5 mmol, 74%) at 4.5°C in two fractions.

^{1}H NMR (400 MHz, C_6D_6): δ = 7.14–7.12 (m, 6H, Ar*H*), 4.79 (s, 2H, C*H*), 3.61 (s, 4H, CH_2CH_2), 3.14 (sept, $^3J_{HH}$ = 6.9 Hz, 4H, C*H*Me$_2$), 1.88 (s, 6H, C*Me*), 1.64 (s, 6H, C*Me*), 1.25-1.21 (m, 18H, CHMe_2 & ZnCH$_2$CH_3), 1.16 (d, $^3J_{HH}$ = 6.9 Hz, 12H, CHMe_2), 0.52 ppm (q, $^3J_{HH}$ = 8.1 Hz, 4H, ZnCH_2CH$_3$); ^{13}C{^{1}H} NMR (101 MHz, C_6D_6): δ = 168.13 (*C*N), 166.42 (*C*N), 145.34 (*i*-C_{arom}), 141.83 (*o*-C_{arom}), 125.87 (*p*-CH_{arom}), 123.76 (*m*-CH_{arom}), 96.44 (*C*H), 54.27 (*C*H_2CH_2), 28.42 (*C*HMe$_2$), 24.43 (CHMe_2), 23.63 (CHMe_2), 23.29 (*C*Me), 22.04 (*C*Me), 12.76 (ZnCH$_2$*C*H$_3$), −1.42 ppm (Zn*C*H$_2$CH$_3$); ATR-IR: $\tilde{\nu}$ = 2959, 2919, 2885, 2848, 1552, 1526, 1508, 1479, 1438, 1381, 1368, 1319, 1307, 1268, 1241, 1184, 1097, 1053, 1016, 1002, 982, 935, 880, 857, 798, 785, 757, 713 cm^{-1}; Anal. calc. (found) for $C_{40}H_{62}N_4Zn_2 \cdot 0.2\,C_7H_8$: C, 66.46 (66.81), H, 8.57 (8.59), N, 7.49 (7.80).

4b: In a pressure Schlenk vessel, $ZnEt_2$ (3.0 mL, 3.3 mmol, 1 M in hexanes) was added dropwise to a stirred solution of **1b** (760 mg, 1.4 mmol) in toluene (8 mL) at 0 °C. Afterwards, the ventil of the vessel was closed and the solution was stirred at room temperature overnight. The yellow solution was filtered and concentrated to the half of the initial volume. **4b** (350 mg, 0.5 mmol, 35%) was obtained from the filtrate as colourless crystals at 4.5°C in two fractions.

^{1}H NMR (400 MHz, C_6D_6): δ = 7.15–7.10 (m, 6H, Ar*H*), 4.81 (s, 2H, C*H*), 3.45–3.41 (m, 4H, CH_2CH$_2$CH_2), 3.13 (sept, $^3J_{HH}$ = 6.9 Hz, 4H, C*H*Me$_2$), 1.89–1.81 (m, 6H, C*Me* & CH$_2$CH_2CH$_2$), 1.65 (s, 6H, C*Me*), 1.27 (t, $^3J_{HH}$ = 8.1 Hz, 6H, ZnCH$_2$CH_3), 1.21 (d, $^3J_{HH}$ = 6.8 Hz, 12H, CHMe_2), 1.15 (d, $^3J_{HH}$ = 6.9 Hz, 12H, CHMe_2), 0.51 ppm (q, $^3J_{HH}$ = 8.1 Hz, 4H, ZnCH_2CH$_3$); ^{13}C{^{1}H} NMR (101 MHz, C_6D_6): δ = 168.00 (*C*N), 166.09 (*C*N), 145.37 (*i*-C_{arom}), 141.82 (*o*-C_{arom}), 125.82 (*p*-CH_{arom}), 123.73 (*m*-CH_{arom}), 96.16 (*C*H), 49.63 (*C*H$_2$CH$_2$CH$_2$), 36.52 (CH$_2$*C*H$_2$CH$_2$), 28.39 (*C*HMe$_2$), 24.36 (CHMe_2), 23.53 (CHMe_2), 23.25 (*C*Me), 21.63 (*C*Me), 12.79 (ZnCH$_2$*C*H$_3$), −1.04 ppm (Zn*C*H$_2$CH$_3$); ATR-IR: $\tilde{\nu}$ = 3058, 2957, 2926, 2867, 2849, 1557, 1523, 1479, 1436, 1399, 1347, 1319, 1269, 1253, 1239, 1196, 1177, 1093, 1054, 1025, 987, 949, 934, 899, 858, 798, 762, 753, 714, 680 cm^{-1}; Anal. calc. (found) for $C_{41}H_{64}N_4Zn_2$: C, 66.21 (66.23), H, 8.67 (8.66), N, 7.53 (7.68).

4c: $ZnEt_2$ (2.8 mL, 2.8 mmol, 1 M in hexanes) was added dropwise to a stirred solution of **1c** (760 mg, 1.3 mmol) in toluene (8 mL) at 0 °C, followed by stirring at room temperature overnight, which yields an orange suspension. The suspension was filtered, and all volatiles of the filtrate were removed in vacuum. The dark orange crude product was recrystallized from toluene (5 mL), filtered, and colourless crystals of **4c** (368 mg, 0.5 mmol, 37%) were obtained upon storage at 4.5°C.

^{1}H NMR (400 MHz, C_6D_6): δ = 7.17–7.12 (m, 6H, Ar*H*), 4.75 (s, 2H, C*H*), 3.96–3.89 (m, 2H, ring-C*H*), 3.17–3.04 (m, 4H, C*H*Me$_2$), 2.15 (s, 6H, C*Me*), 1.85–1.81 (br, 2H, ring-CH_2), 1.71-1.65 (br, 2H, ring-CH_2), 1.63 (s, 6H, C*Me*), 1.61–1.55 (br, 2H, ring-CH_2), 1.31 (d, $^3J_{HH}$ = 6.8 Hz, 6H, CHMe_2), 1.29–1.26 (br, 2H, ring-CH_2), 1.25–1.19 (m, 12H, CHMe_2 & ZnCH$_2$CH_3), 1.12 (dd, $^3J_{HH}$ = 6.9 & 1.3 Hz, 12H, CHMe_2), 0.62–0.48 ppm (m, 4H, ZnCH_2CH$_3$); ^{13}C{^{1}H} NMR (101 MHz, C_6D_6): δ = 166.54 (*C*N), 166.08 (*C*N), 145.50 (*i*-C_{arom}), 141.88 (*o*-C_{arom}), 141.84 (*o*-C_{arom}), 125.80 (*p*-CH_{arom}), 123.81 (*m*-CH_{arom}), 123.70 (*m*-CH_{arom}), 95.93 (*C*H), 65.71 (ring-*C*H), 36.52 (ring-*C*H_2), 28.53 (*C*HMe$_2$), 28.35 (*C*HMe$_2$), 25.44 (ring-*C*H_2), 24.57 (*C*Me), 24.47 (CHMe_2), 24.22 (CHMe_2), 23.95 (CHMe_2), 23.69 (CHMe_2), 23.08 (*C*Me), 12.81 (ZnCH$_2$*C*H$_3$), 3.35 ppm (Zn*C*H$_2$CH$_3$); ATR-IR: $\tilde{\nu}$ = 2959, 2924, 2854, 1550, 1523, 1455, 1436, 1382, 1347, 1318, 1274, 1253, 1242, 1189, 1096, 1024, 995, 957, 934, 883, 857, 796, 760, 746, 715, 670 cm^{-1}; Anal. calc. (found) for $C_{44}H_{68}N_4Zn_2 \cdot 0.7\,C_5H_{12}$: C, 68.38 (68.49), H, 9.23 (9.07), N, 6.72 (6.71).

4f: $ZnEt_2$ (3.3 mL, 3.3 mmol, 1 M in hexanes) was added dropwise to a stirred solution of **1f** (730 mg, 1.5 mmol) in toluene (6 mL) at 0 °C. After stirring the orange-red solution at room temperature overnight, all volatiles were removed in vacuum. The red brown crude product was recrystallized from toluene (5 mL), filtered, and concentrated to the half of the initial volume. **4f** (472 mg, 0.7 mmol, 47%) was obtained from the filtrate as colourless crystals at −25°C.

^{1}H NMR (400 MHz, C_6D_6): δ = 7.10–6.95 (m, 6H, Ar*H*), 4.65 (s, 2H, C*H*), 3.88–3.75 (m, 2H, ring-C*H*), 2.10 (d, $^3J_{HH}$ = 2.7 Hz, 12H, Ar*Me*), 2.04 (s, 6H, C*Me*), 1.80–1.70 (br, 2H, ring-CH_2), 1.65–1.52 (br, 4H, ring-CH_2), 1.49 (s, 6H, C*Me*), 1.29–1.20 (m, 8H, ring-CH_2 & ZnCH$_2$CH_3), 0.62-0.44 ppm (m, 4H, ZnCH_2CH$_3$); ^{13}C{^{1}H} NMR (101 MHz, C_6D_6): δ = 166.32 (*C*N), 165.08 (*C*N), 148.56 (*i*-C_{arom}), 131.67 (*o*-C_{arom}), 131.64 (*o*-C_{arom}), 128.58 (*m*-CH_{arom}), 128.50 (*m*-CH_{arom}), 124.75 (*p*-CH_{arom}), 95.87 (*C*H), 66.03 (ring-*C*H), 36.10 (ring-*C*H_2), 25.48 (ring-*C*H_2), 24.25 (*C*Me), 22.22 (*C*Me), 18.92 (Ar*Me*), 18.80 (Ar*Me*), 12.70 (ZnCH$_2$*C*H$_3$), 2.83 ppm (Zn*C*H$_2$CH$_3$); ATR-IR:

$\tilde{\nu}$ = 2941, 2900, 2840, 1545, 1523, 1442, 1383, 1342, 1317, 1272, 1240, 1201, 1092, 1077, 1026, 1011, 982, 947, 889, 853, 800, 763, 744, 671 cm^{-1}; Anal. calc. (found) for $C_{36}H_{52}N_4Zn_2$: C, 64.38 (64.64), H, 7.80 (7.69), N, 8.34 (8.36).

5a and 6a: Under inert conditions, $ZnEt_2$ (3.0 mL, 3.0 mmol, 1 M in hexanes) was added dropwise to a stirred solution of **1a** (740 mg, 1.4 mmol) in toluene (7 mL) at room temperature, followed by stirring at room temperature for 3 h. After gas evolution was complete, the bubble counter was replaced by a drying tube filled with orange gel and the yellow solution was stirred at room temperature for additional 5 days. Under inert conditions, all volatiles of the solution were removed in vacuum, the crude product was recrystallized from *n*-hexane (10 mL) and filtered. **5a** (110 mg, 0.1 mmol, 13%) was obtained from the filtrate as colourless crystals at 4.5°C in the first fraction, while colourless crystals of **6a** (100 mg, 0.1 mmol, 14%) were obtained in the second fraction at −25°C.

5a: Due to the complexity of the ^{1}H NMR spectra (C_6D_6 and THF-d_8), no assignment of the signals could be performed; ATR-IR: $\tilde{\nu}$ = 3674, 3072, 2960, 2924, 2864, 1552, 1523, 1508, 1465, 1436, 1403, 1382, 1355, 1333, 1319, 1262, 1253, 1238, 1191, 1098, 1054, 1017, 935, 883, 850, 795, 760, 747, 734, 713 cm^{-1}; Anal. calc. (found) for $C_{84}H_{136}N_8O_8Zn_2$: C, 56.37 (56.56), H, 7.71 (7.66), N, 6.30 (6.26).

6a: ^{1}H NMR (400 MHz, C_6D_6): δ = 7.19–7.13 (m, 6H, Ar*H*), 4.70 (s, 2H, C*H*), 4.03–3.94 (m, 2H, OCH_2CH$_3$), 3.59–3.31 (m, 8H, C*H*Me$_2$ & CH_2CH_2), 1.70 (s, 12H, C*Me*), 1.45 (s, 3H, OC(O)CH_3), 1.38–1.34 (m, 15H, CH*Me*$_2$ & OCH$_2$CH_3), 1.28 (d, $^3J_{HH}$ = 6.9 Hz, 6H, CH*Me*$_2$), 1.19 ppm (d, $^3J_{HH}$ = 6.9 Hz, 6H, CH*Me*$_2$); ^{13}C{^{1}H} NMR (101 MHz, C_6D_6): δ = 181.23 (O*C*(O)CH$_3$), 169.02 (*C*N), 167.37 (*C*N), 144.81 (*i*-C_{arom}), 143.52 (*o*-C_{arom}), 142.95 (*o*-C_{arom}), 125.61 (*p*-CH_{arom}), 123.97 (*m*-CH_{arom}), 123.76 (*m*-CH_{arom}), 94.24 (*C*H), 62.41 (O*C*H$_2$CH$_3$), 53.20 (*C*H$_2$*C*H$_2$), 28.13 (*C*HMe$_2$), 28.08 (*C*HMe$_2$), 25.31 (CH*Me*$_2$), 24.74 (CH*Me*$_2$), 24.42 (CH*Me*$_2$), 24.29 (CH*Me*$_2$), 23.82 (*C*Me), 22.65 (OC(O)*C*H$_3$), 22.59 (*C*Me), 20.52 ppm (OCH$_2$*C*H$_3$); ATR-IR: $\tilde{\nu}$ = 3063, 2961, 2927, 2866, 1597, 1574, 1547, 1511, 1462, 1435, 1402, 1376, 1317, 1264, 1254, 1239, 1193, 1101, 1055, 1021, 936, 878, 796, 760, 747, 738, 716, 667 cm^{-1}; Anal. calc. (found) for $C_{40}H_{60}N_4O_3Zn_2 \cdot 0.1\,C_6H_{14}$: C, 62.17 (62.37), H, 7.89 (7.90), N, 7.14 (7.39).

5b: Under inert conditions, $ZnEt_2$ (3.0 mL, 3.0 mmol, 1 M in hexanes) was added dropwise to a stirred solution of **1b** (760 mg, 1.4 mmol) in toluene (7 mL) at room temperature, followed by stirring at room temperature for 3 h. After gas evolution was complete, the bubble counter was replaced by a drying tube filled with orange gel and the yellow solution was stirred at room temperature for additional 5 days. Under inert conditions, all volatiles of the solution were removed in vacuum, the crude product was recrystallized from *n*-hexane (10 mL) and hot filtered. Slowly cooling down to room temperature, affording colourless crystals of **5b** (390 mg, 0.5 mmol, 37%) from the light orange solution.

^{1}H NMR (300 MHz, C_6D_6): δ = 7.13–7.11 (m, 6H, Ar*H*), 4.66 (s, 2H, C*H*), 3.89 (q, $^3J_{HH}$ = 6.9 Hz, 4H, OCH_2CH$_3$), 3.43 (sept, $^3J_{HH}$ = 6.8 Hz, 4H, C*H*Me$_2$), 3.29 (t, $^3J_{HH}$ = 6.3 Hz, 4H, CH_2CH$_2$CH_2), 2.15 (quint, $^3J_{HH}$ = 6.2 Hz, 2H, CH$_2$CH_2CH$_2$), 1.80 (s, 6H, C*Me*), 1.68 (s, 6H, C*Me*), 1.19–1.13 ppm (m, 30H, CH*Me*$_2$ & OCH$_2$CH_3); ^{13}C{^{1}H} NMR (75 MHz, C_6D_6): δ = 168.51 (*C*N), 166.66 (*C*N), 145.36 (*i*-C_{arom}), 142.89 (*o*-C_{arom}), 125.31 (*p*-CH_{arom}), 123.76 (*m*-CH_{arom}), 94.21 (*C*H), 61.46 (O*C*H$_2$CH$_3$), 48.63 (*C*H$_2$CH$_2$*C*H$_2$), 31.21 (CH$_2$*C*H$_2$CH$_2$), 28.00 (*C*HMe$_2$), 24.51 (CH*Me*$_2$), 24.31 (CH*Me*$_2$), 23.96 (*C*Me), 22.18 (*C*Me), 21.31 ppm (OCH$_2$*C*H$_3$); ATR-IR: $\tilde{\nu}$ = 2956, 2922, 2854, 1579, 1548, 1507, 1436, 1397, 1380, 1343, 1312, 1253, 1243, 1191, 1105, 1055, 1016, 983, 933, 882, 857, 816, 794, 758, 744, 714, 670 cm^{-1}; Anal. calc. (found) for $C_{41}H_{64}N_4O_2Zn_2$: C, 63.48 (63.86), H, 8.32 (8.18), N, 7.22 (7.14).

7a: Under inert conditions, **4a** (500 mg, 0.7 mmol) was dissolved in toluene (7 mL) at room temperature. Afterwards the glass stopper was replaced by a drying tube filled with orange gel and the yellow solution was stirred at room temperature for 13 days. Under inert conditions, all volatiles of the dark yellow solution were removed in vacuum, the crude product was dissolved in *n*-hexane (8 mL) and filtered. The filtrate was concentrated to three-quarters of the initial volume, and very few colourless crystals of **3a** and **7a** were obtained upon storage at −25°C, which could not be further analyzed.

Due to the complexity of the ^{1}H & ^{13}C{^{1}H} NMR spectra (C_6D_6), no assignment of the signals could be performed; ATR-IR: $\tilde{\nu}$ = 3699, 3649, 2961, 2926, 2865, 1583, 1558, 1514, 1481, 1461, 1437, 1395, 1342, 1324, 1308, 1283, 1264, 1254, 1238, 1190, 1094, 1056, 1017, 937, 880, 847, 833, 794, 759, 730, 717 cm^{-1}; elemental analysis could not be performed due to an insufficient amount of sample.

Acknowledgements

The project was financially supported by the *Fonds der Chemischen Industrie*, the *Deutsche Forschungsgemeinschaft* (DFG, KR4782/3-1) and the Friedrich-Schiller-Universität Jena. Generous support from Professor Manfred Scheer is gratefully acknowledged. The authors are thankful for valuable comments by the reviewers that helped improving the quality of the manuscript. Open Access funding enabled and organized by Projekt DEAL.

Data Availability Statement

The data that support the findings of this study are available in the supplementary material of this article.

References

[1] E. von Frankland, *Justus Liebigs Ann. Chem.* **1849**, *71*, 171–213.
[2] P. Barbier, *Compt. Rend.* **1899**, *128*, 110.
[3] S. Reformatsky, *Ber. Dtsch. Chem. Ges.* **1887**, *20*, 1210–1211.
[4] S. Enthaler, X.-F. Wu (Eds.) *Zinc catalysis*. Applications in organic synthesis, Wiley-VCH, Verlag GmbH & Co. KGaA, Weinheim, Germany, **2015**.
[5] X.-F. Wu, H. Neumann, *Adv. Synth. Catal.* **2012**, *354*, 3141–3160.
[6] P. Dubois, O. Coulembier, J.-M. Raquez, *Handbook of ring-opening polymerization*, Wiley-VCH, Weinheim, **2009**.
[7] X.-F. Wu, *Chem. Asian J.* **2012**, *7*, 2502–2509.
[8] a) M. F. Pilz, C. Limberg, B. B. Lazarov, K. C. Hultzsch, B. Ziemer, *Organometallics* **2007**, *26*, 3668–3676; b) M. R. Kember, P. D. Knight, P. T. R. Reung, C. K. Williams, *Angew. Chem. Int. Ed.* **2009**, *48*, 931–933; *Angew. Chem.* **2009**, *121*, 949–951; c) A. Buchard, F. Jutz, M. R. Kember, A. J. P. White, H. S. Rzepa, C. K. Williams, *Macromolecules* **2012**, *45*, 6781–6795; d) M. W. Lehenmeier, S. Kissling, P. T. Altenbuchner, C. Bruckmeier, P. Deglmann, A.-K. Brym, B. Rieger, *Angew. Chem. Int. Ed.* **2013**, *52*, 9821–9826; *Angew. Chem.* **2013**, *125*, 10004–10009; e) W.-L. Kong, Z.-X. Wang, *Dalton Trans.* **2014**, *43*, 9126–9135; f) A. Thevenon, J. A. Garden, A. J. P. White, C. K. Williams, *Inorg. Chem.* **2015**, *54*, 11906–11915; g) C. Romain, M. S. Bennington, A. J. P. White, C. K. Williams, S. Brooker, *Inorg. Chem.* **2015**, *54*, 11842–11851.
[9] a) R. Peters (Ed.) *Cooperative Catalysis: Designing Efficient Catalysts for Synthesis*, Wiley, **2015**; b) P. Kalck, *Homo- and Heterobimetallic Complexes in Catalysis*, Springer International Publishing, Cham, **2016**.
[10] R. Kretschmer, *Chem. Eur. J.* **2020**, *26*, 2099–2119.
[11] a) D. F.-J. Piesik, S. Range, S. Harder, *Organometallics* **2008**, *27*, 6178–6187; b) S. Kissling, M. W. Lehenmeier, P. T. Altenbuchner, A. Kronast, M. Reiter, P. Deglmann, U. B. Seemann, B. Rieger, *Chem. Commun.* **2015**, *51*, 4579–4582; c) S. Kissling, P. T. Altenbuchner, M. W. Lehenmeier, E. Herdtweck, P. Deglmann, U. B. Seemann, B. Rieger, *Chem. Eur. J.* **2015**, *21*, 8148–8157.
[12] M. Köhler, P. Rinke, K. Fiederling, H. Görls, N. Ueberschaar, F. H. Schacher, R. Kretschmer, *Macromol. Chem. Phys.* **2021**, *222*, 2100187.
[13] Y. Li, Y. Dang, D. Li, H. Pan, L. Zhang, L. Wang, Z. Cao, Y. Li, *Organometallics* **2021**, *40*, 482–489.
[14] T. Pietrzak, M. D. Korzyński, I. Justyniak, K. Zelga, A. Kornowicz, Z. Ochal, J. Lewiński, *Chem. Eur. J.* **2017**, *23*, 7997–8005.
[15] a) D. V. Vitanova, F. Hampel, K. C. Hultzsch, *J. Organomet. Chem.* **2005**, *690*, 5182–5197; b) S. Gong, H. Ma, J. Huang, *Dalton Trans.* **2009**, 8237–8247; c) I. El-Zoghbi, T. J. J. Whitehorne, F. Schaper, *Dalton Trans.* **2013**, *42*, 9376–9387; d) A. Phanopoulos, A. H. M. Leung, S. Yow, D. Palomas, A. J. P. White, K. Hellgardt, A. Horton, M. R. Crimmin, *Dalton Trans.* **2017**, *46*, 2081–2090; e) M. E. Desat, R. Kretschmer, *Chem. Eur. J.* **2018**, *24*, 12397–12404; f) O. Kysliak, H. Görls, R. Kretschmer, *J. Am. Chem. Soc.* **2021**, *143*, 142–148.
[16] M. Cheng, D. R. Moore, J. J. Reczek, B. M. Chamberlain, E. B. Lobkovsky, G. W. Coates, *J. Am. Chem. Soc.* **2001**, *123*, 8738–8749.
[17] a) D. Seyferth, *Organometallics* **2001**, *20*, 2940–2955; b) D. Prochowicz, K. Sokołowski, J. Lewiński, *Coord. Chem. Rev.* **2014**, *270–271*, 112–126.
[18] M. E. Desat, R. Kretschmer, *Dalton Trans.* **2019**, *48*, 17718–17722.
[19] D. M. Ermert, I. Ghiviriga, V. J. Catalano, J. Shearer, L. J. Murray, *Angew. Chem. Int. Ed.* **2015**, *54*, 7047–7050; *Angew. Chem.* **2015**, *127*, 7153–7156.
[20] a) J. Lewiński, W. Marciniak, J. Lipkowski, I. Justyniak, *J. Am. Chem. Soc.* **2003**, *125*, 12698–12699; b) J. Lewiński, W. Sliwiński, M. Dranka, I. Justyniak, J. Lipkowski, *Angew. Chem. Int. Ed.* **2006**, *45*, 4826–4829; *Angew. Chem.* **2006**, *118*, 4944–4947; c) J. Lewiński, K. Suwała, M. Kubisiak, Z. Ochal, I. Justyniak, J. Lipkowski, *Angew. Chem. Int. Ed.* **2008**, *47*, 7888–7891; *Angew. Chem.* **2008**, *120*, 8006–8009; d) J. Lewiński, K. Suwała, T. Kaczorowski, M. Gałezowski, D. T. Gryko, I. Justyniak, J. Lipkowski, *Chem. Commun.* **2009**, 215–217; e) K. Zelga, M. Leszczyński, I. Justyniak, A. Kornowicz, M. Cabaj, A. E. H. Wheatley, J. Lewiński, *Dalton Trans.* **2012**, *41*, 5934–5938; f) P. Sobota, R. Petrus, K. Zelga, L. Mąkolski, D. Kubicki, J. Lewiński, *Chem. Commun.* **2013**, *49*, 10477–10479; g) L. Mąkolski, K. Zelga, R. Petrus, D. Kubicki, P. Zarzycki, P. Sobota, J. Lewiński, *Chem. Eur. J.* **2014**, *20*, 14790–14799; h) M. K. Leszczyński, I. Justyniak, J. Lewiński, *Organometallics* **2017**, *36*, 2377–2380.
[21] a) J. Lewiński, M. Kościelski, K. Suwała, I. Justyniak, *Angew. Chem. Int. Ed.* **2009**, *48*, 7017–7020; *Angew. Chem.* **2009**, *121*, 7151–7154; b) T. Pietrzak, I. Justyniak, M. Kubisiak, E. Bojarski, J. Lewiński, *Angew. Chem. Int. Ed.* **2019**, *58*, 8526–8530; *Angew. Chem.* **2019**, *131*, 8614–8618.
[22] D. R. Moore, M. Cheng, E. B. Lobkovsky, G. W. Coates, *J. Am. Chem. Soc.* **2003**, *125*, 11911–11924.
[23] S. Schulz, T. Eisenmann, D. Bläser, R. Boese, *Z. Anorg. Allg. Chem.* **2009**, *635*, 995–1000.
[24] S. Gondzik, S. Schulz, D. Bläser, C. Wölper, *Chem. Commun.* **2014**, *50*, 1189–1191.
[25] H.-Y. Chen, Y.-L. Peng, T.-H. Huang, A. K. Sutar, S. A. Miller, C.-C. Lin, *J. Mol. Catal. A* **2011**, *339*, 61–71.
[26] a) K. Sokołowski, W. Bury, I. Justyniak, A. M. Cieślak, M. Wolska, K. Sołtys, I. Dzięcielewski, J. Lewiński, *Chem. Commun.* **2013**, *49*, 5271–5273; b) K. Sokołowski, W. Bury, I. Justyniak, D. Fairen-Jimenez, K. Sołtys, D. Prochowicz, S. Yang, M. Schröder, J. Lewiński, *Angew. Chem. Int. Ed.* **2013**, *52*, 13414–13418; *Angew. Chem.* **2013**, *125*, 13656–13660; c) K. Sokołowski, W. Bury, A. Tulewicz, A. M. Cieślak, I. Justyniak, D. Kubicki, E. Krajewska, A. Milet, R. Moszyński, J. Lewiński, *Chem. Eur. J.* **2015**, *21*, 5496–5503.
[27] D. Schröder, H. Schwarz, S. Schenk, E. Anders, *Angew. Chem. Int. Ed.* **2003**, *42*, 5087–5090; *Angew. Chem.* **2003**, *115*, 5241–5244.
[28] a) N. Dietl, M. Schlangen, H. Schwarz, *Angew. Chem. Int. Ed.* **2012**, *51*, 5544–5555; *Angew. Chem.* **2012**, *124*, 5638–5650; b) H. Schwarz, *Chem. Phys. Lett.* **2015**, *629*, 91–101.

Manuscript received: February 26, 2023
Revised manuscript received: March 15, 2023
Version of record online: April 7, 2023